

Effect of Fe²⁺ Substitution on Structural, Functional, and Optical Properties of Nano TiO₂ Prepared Via Sol-Gel Method

C. Gnana Sambandam*

*(Physics Research Centre, S.T. Hindu College, Nagercoil-2, Tamilnadu, India.)

ABSTRACT

Nanoparticles of titanium dioxide doped with Fe²⁺ ions have been prepared through an aqueous sol-gel technique using titanium tetra isopropoxide (TTIP) and ferrous sulphate as a precursor. The mesoporous nature of both pure and Fe²⁺ doped TiO₂ powders, with specific surface area of 7.4 and 6.6 m² g⁻¹, respectively, is maintained even at calcination temperature of to 550⁰C. The synthesized Nano powders were characterized by Powder X-ray Diffraction (PXRD), Scanning Electron Microscope (SEM), Fourier Transform Infrared (FTIR), Ultraviolet Visible (UV-Vis) and Photoluminescence (PL) Spectroscopy. PXRD pattern indicates the presence of pure crystalline anatase phase TiO₂ with average crystallite size of 14 nm. FTIR spectra showed the vibrational bands of Ti-O networks. The morphology of the as prepared samples and chemical constituents of the nanoparticles studied using SEM and EDAX analysis. From the UV-Vis spectra and PL spectra the optical properties of TiO₂ were studied and discussed.

Keywords - sol-gel, Nano TiO₂, Fe doping, SEM, EDAX

I. INTRODUCTION

In recent years, intense effect has been focused on preparation of metal oxide Nano crystals owing to their markedly different physical and chemical properties with respect to the bulk materials. Particularly titanium dioxide, TiO₂, has been studied extensively as photo catalyst to deal with environment pollution, water purification, wastewater treatment, hazardous waste control and air purification [1-5]. Titanium dioxide (TiO₂) is of great interest in technological applications due to its morphology and crystalline phase. TiO₂ exists three different phases, i.e., anatase, rutile, and Brookite. The active crystallite phases of TiO₂ are anatase and rutile [6,7]. TiO₂ has been widely studied regarding various applications, utilizing the photo catalytic and transparent conductivity, which strongly depend on the crystalline structure, morphology and crystallite size [8]. TiO₂ nanoparticles have been prepared by different methods such as, chemical precipitation method [9], chemical vapors deposition (CVD) [10], the sol-gel technique [11], sputtering [12], hydrolysis, micro emulsion method [13], spray deposition [14], aerosol-assisted chemical vapor deposition [15], thermal plasma [16], hydrothermal method [17], microwave assisted hydrothermal synthesis [18], solvothermal method [19] and flame combustion method [20]. Among these methods sol-gel method is a simple method to synthesis TiO₂ nanoparticles. Researchers used lot of organic solvents like toluene [21], ethanol [22] for preparing Nano TiO₂ in various methods.

In this study we have prepared TiO₂ via sol-gel method using isopropanol as a solvent. The products were characterized by Powder X-ray Diffraction, Fourier Transform Infrared Spectroscopy, Scanning Electron Microscope, Energy Dispersive Spectroscopy, UV-Vis spectra and Photoluminescence studies.

II. EXPERIMENTAL

2.1 Materials

Titanium tetraisopropoxide (TTIP, 97%, Sigma Aldrich), Isopropyl alcohol (RANKEM), Deionised water.

2.2 Synthesis of TiO₂ nanoparticles

TiO₂ Nano powders were prepared via sol-gel method using the precursor Titanium isopropoxide (TTIP, 97%, Sigma Aldrich), Deionised water and Isopropyl alcohol (RANKEM) as the starting materials. 100 ml of Isopropyl alcohol was added to 15 ml of TTIP in 200ml beaker. The mixture solution is stirred 10 minutes using magnetic stirrer. For hydrolysis reaction 10 ml of deionised water was added drop wise to the mixed solution. Then the mixture solution was stirred continuously for 2 hours. Now the mixture transformed to gel. After aging 24 hours the gel is filtered and dried. For doping purpose suitable amount of Fe metal dopant taken in the hydrolysis step. The dried Nano TiO₂ is calcinated to 550⁰C. During the preparation the p^H of the mixed solution maintained in the acidity range.

2.2 Material Characterization

The prepared Nano TiO₂ were characterized by Powder XRD using XPERTPRO diffractometer. FTIR spectra of the as prepared Nano TiO₂ were characterized by Jasco 4100 Spectro Photometer equipped with ATR. UV-Vis absorption spectra of the as prepared nano TiO₂ samples were recorded using UV-2401 PC UV-Vis recording Spectrophotometer. The Photoluminescence spectra of the as prepared Nano TiO₂ samples were recorded using VARIAN-CARY Eclipse Fluorescence Spectrophotometer. SEM-EDAX spectra of Nano TiO₂ were recorded using FEI Quanta FEG 200-High Resolution Scanning Electron Microscope.

III. RESULTS AND DISCUSSION

3.1 Powder XRD Analysis

Figure(1) shows the Powder X-Ray Diffraction patterns of as prepared undoped TiO₂, 2 wt% Fe-doped TiO₂, 3 wt% Fe-doped TiO₂ and 5 wt% Fe-doped TiO₂ Nano powders. The 2θ scans were recorded at several resolutions using Cu Kα-1 radiation of wavelength 1.54060 Å range 20-80°. The Powder X-Ray Diffraction patterns of the as prepared TiO₂ showed the presence of broad peaks. The broad peaks indicate either particles of very small crystalline size, or particles are semi crystalline in nature [23].

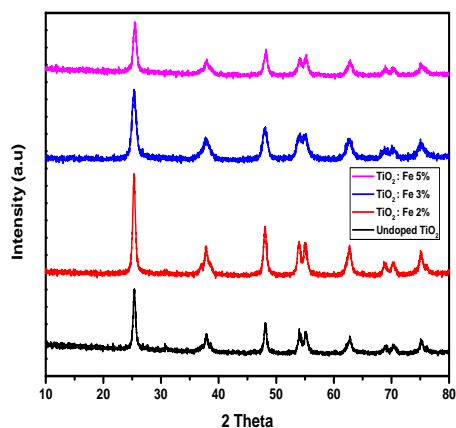


Fig -1: XRD patterns of as prepared undoped and Fe-doped Nano particles

All the diffraction lines are assigned to anatase crystalline phase of titanium dioxide. The Powder X-Ray Diffraction pattern is in excellent agreement with a reference pattern (JCPDS 21-1272) of titanium dioxide. It should be noted that only anatase TiO₂ can be found in this sample, which is attributed to the contribution of the low concentration of oxygen vacancies due to high concentration of gaseous oxygen during particle growth, hindering the transformation from anatase to rutile phase [24]. With increasing Fe loading the intensity of the peaks

relatively reduced and with highest Fe loading they are broadened [25]. From Powder X-Ray Diffraction results, the crystallite size can be estimated from width of the peak through use of Scherrer equation: $D = K \lambda / \beta \cos \theta$, where D is the crystallite size, λ is the wavelength of X-ray radiation (Cu Kα-1 radiation = 1.54060 Å), K is a constant and usually taken as 0.9, β is the full width at half maximum (FWHM) after subtraction of equipment broadening, and θ is the Bragg angle of the peak [26]. The sample are typical anatase titania crystal structure (21-1272) with peaks at 2θ of 25.3, 37.9, 48.1, 53.9, 55.0, 62.8, 68.9, 70.41 and 75.18 corresponding to (101), (004), (200), (105), (211), (204), (116), (220) and (215) phases respectively [27]. From the Powder XRD spectrum the average crystallite size is found to be 14-21 nm.

Yin Zhao and co-workers obtained the same result previously by preparing TiO₂ Nano powders by a facile gas flame combustion method using Titanium Chloride as a precursor [28].

3.2 FTIR Analysis

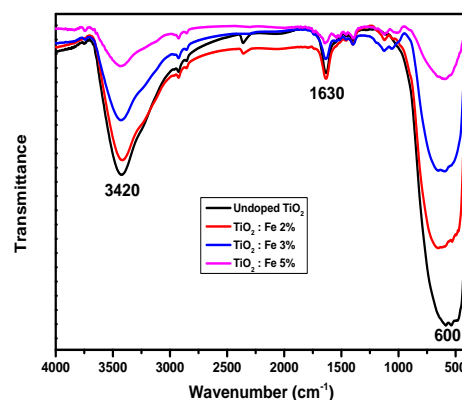


Fig -2: FTIR spectrum of the as prepared undoped and Fe-doped Nano particles.

The FTIR spectra of the as prepared undoped and Fe-doped Nano TiO₂ are shown in figure (2). From this spectrum, it can be observed apparently that strong band in the range of 580 to 660 cm⁻¹ is associated with the characteristic modes of TiO₂. The absorption range around 3400cm⁻¹ indicates that the presence of hydroxyl (stretching), which is probably due to the fact that the spectra were recorded in situ and some reabsorptions of water from the ambient atmosphere has occurred [29]. The absorption range around 1630 cm⁻¹ may be related to hydroxyl (bending) groups of molecular water [20].

3.3 UV-Vis Analysis

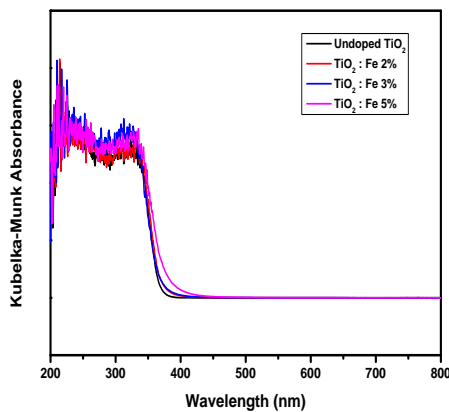


Fig -3: UV-Vis DRS spectrum of the as prepared undoped and Fe-doped nanoparticles.

Figure (3) shows the plots of the Kubelka-Munk function $F(R_{\infty})$ vs wavelength obtained from Diffuse Reflectance Spectra data similarly as observed by Shi-An Gao et.al [30].

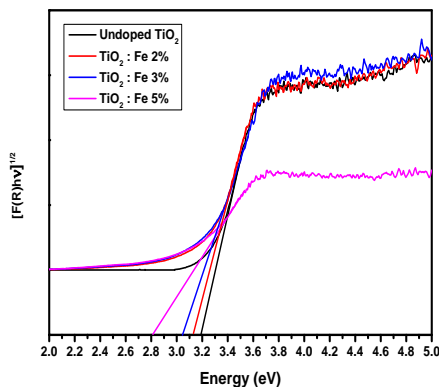


Fig -4: Tauc plot obtained from UV-Vis DRS spectrum of the as prepared undoped and Fe-doped Nano particles.

Figure (4) shows the Tauc plot for the observed Diffuse Reflectance Spectral data for determining band gap energies, E_g . we followed the calculation procedure of Beranek and Kisch [31], who used the equation $\alpha = A(h\nu - E_g)^n/h\nu$, where α is absorption coefficient, A is constant, $h\nu$ is the energy of light and n is a constant depending on the nature of the electron transition [32]. Assuming an indirect band gap ($n=2$) for TiO₂ [33], with α proportional to $F(R_{\infty})$ the band gap energy can be obtained from the plots of $[F(R_{\infty}) hv]^{1/2}$ vs $h\nu$ as the intercept at $[F(R_{\infty}) hv]^{1/2} = 0$ the extrapolated linear part of the plot (fig1). The band gap of undoped and Fe-doped nano TiO₂ obtained from Tauc plot is 2.8 to 3.2 eV.

3.4 SEM Micrograph Analyses

Figure (5), (6),(7) and (8) shows the HR-SEM images of the as prepared and Fe-doped Nano TiO₂.

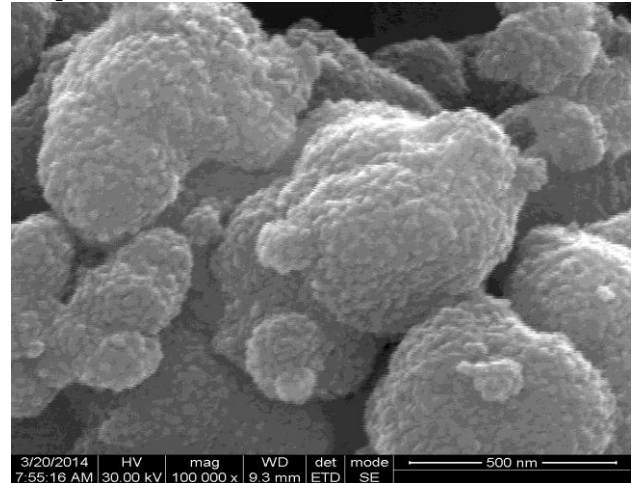


Fig -5: HR-SEM micrographs of the as prepared TiO₂ nanoparticles.

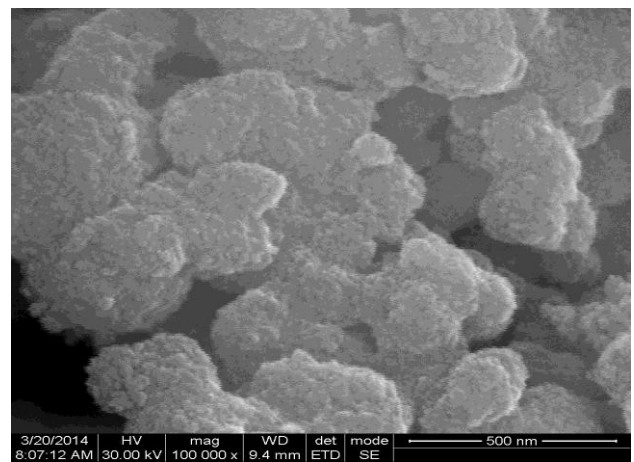


Fig -6: HR-SEM micrograph of the 2 wt% Fe-doped TiO₂ nanoparticles.

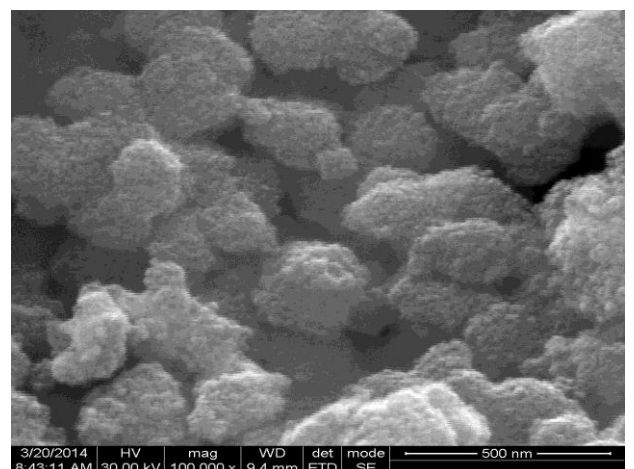


Fig -7: HR-SEM micrograph of the 3 wt% Fe-doped TiO₂ nanoparticles.

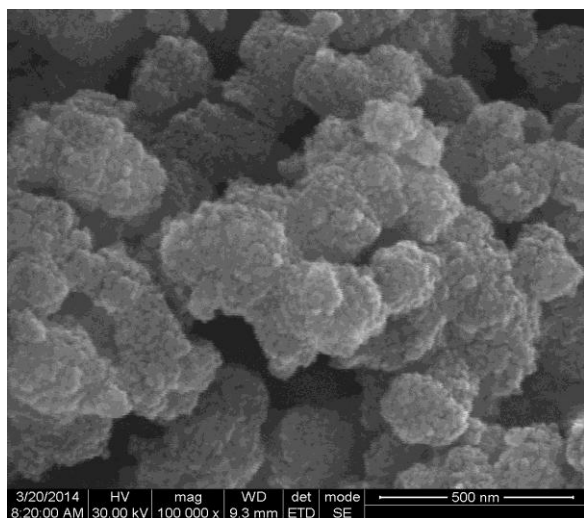


Fig -8: HR-SEM micrographs of the 5 wt% Fe-doped TiO₂ nanoparticles.

The surface morphology of TiO₂ Nano TiO₂ has been studied using High Resolution Scanning Electron Microscope. As the calcination temperature increase, the particles agglomerate resulting in increase of particle size. It is observed from the HR-SEM images. The HR-SEM investigations of all the Nano TiO₂ samples reveal that the crystallites are Nano meter size. Therefore the growth of Nano phase crystalline TiO₂ particles is accelerated at higher calcination temperature [34]. All samples shows uniform morphology in the form of TiO₂ Nano clusters.

3.5 EDAX Analysis

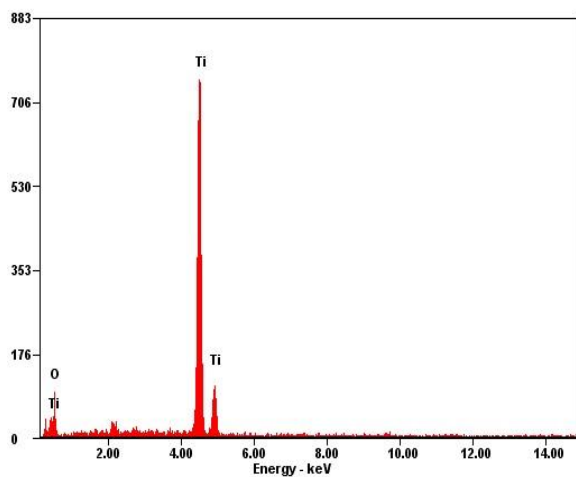


Fig -9: EDAX spectrum of the as prepared Nano TiO₂.

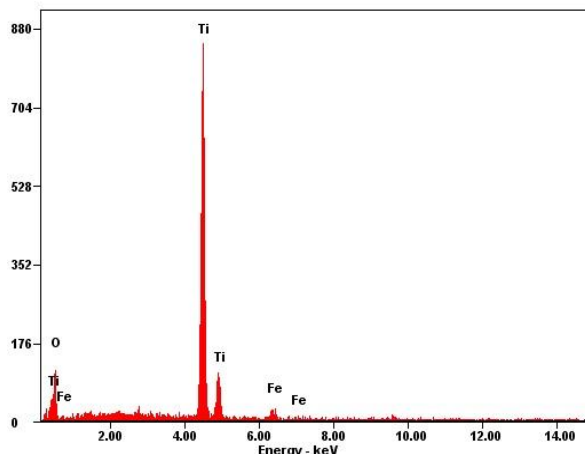


Fig -10: EDAX spectrum of the 2 wt% Fe-doped Nano TiO₂.

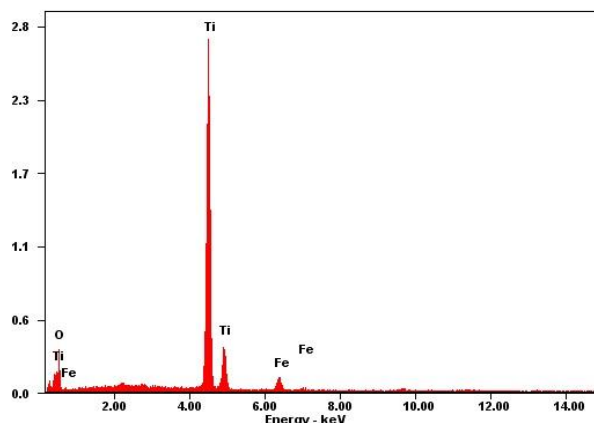


Fig -11: EDAX spectrum of the 3 wt% Fe-doped nano TiO₂.

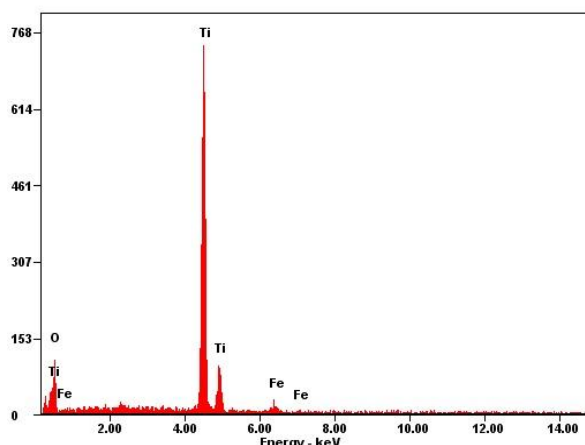


Fig -12: EDAX spectrum of the 5 wt% Fe-doped nano TiO₂.

Figure (9), (10),(11) and (12) shows the EDAX spectrum of as prepared undoped and Fe-

doped Nano TiO₂. The spectrum shows the chemical constituents of Ti, O and Fe present in the samples. There is no impurity peak is observed in the EDAX spectra. This confirms that the prepared samples are in pure form.

3.6 PL Analysis

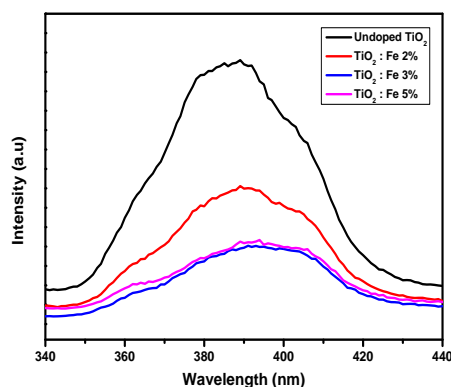


Fig -13: The Photoluminescence spectrum of as

Prepared undoped and Fe-doped Nano TiO₂. Photoluminescence spectra were recorded at room temperature on the prepared Nano TiO₂ prepared by sol-gel synthesis. The Photoluminescence spectra of the prepared undoped and Fe-doped Nano TiO₂ shown in figure (13).

The Photoluminescence spectrum of anatase phase nanoTiO₂ resulted from three origins: self trapped excitons [35,37] surface states [36] and oxygen vacancies [35,37]. Oxygen vacancy peaks normally observed at 391nm and 409 nm. In our samples, all the peaks observed around 390 nm. This shows the Photoluminescence emission due to the presence of oxygen vacancies of Nano TiO₂.

IV. CONCLUSIONS

TiO₂ Nano powders were successfully synthesized by sol-gel method using Titanium tetra isopropoxide and Isopropanol. They were calcinated to 550°C to get high degree of crystallization. The calcinated TiO₂ Nano powders were characterized by Powder XRD, FTIR, SEM, EDS and PL analysis. The Powder XRD spectra reveal that, the main phase of TiO₂ Nano powders are anatase phase. FTIR spectra displayed the peaks attributed to the presence of O-H groups at 3420 cm⁻¹ and 1630 cm⁻¹. Also FTIR spectra show the vibrational mode of TiO₂ around 600 cm⁻¹. SEM image displayed the uniform morphology in the form of Nano clusters. EDAX spectra confirm the samples are in pure form. From UV-Vis Tauc plot the band gap of TiO₂ changes from 2.8-3.2 eV. PL spectra reveal that PL excitation is due to oxygen vacancies.

V. ACKNOWLEDGEMENTS

This work was supported by University Grant Commission, New Delhi, through the Minor Research Project (XII PLAN) in S. T. Hindu College Nagercoil, Tamilnadu, India.

REFERENCES

- [1]. U. Diebold, *Surf. Sci. Rep.* 48(2003) 53.
- [2]. A. Mills, S. Le Hunte, *J. Photochem Photobiol. A* 108 (1997) 1.
- [3]. Y. Ohko, I. Ando, C. Niwa, T. Tatsuma, T. Yamamura, T. Nakashima, Y. Kubota, A. Fujishima, *Environ. Sci. Technol.* 35 (2001) 2635.
- [4]. J. Rodriguez, T. Jirsak, G. Liu, J. Herbek, J. Dvorak, A. Maiti. *J. Am. Chem. Soc.* 123 (2001) 9597.
- [5]. J. Aguado, R. Van Grieken, M.J. Lopez-Munoz, J. Murugan, *Catal. Today* 75 (2002) 95.
- [6]. K. Joseph Antony Raj, B. Vishwanathan, Effect of surface area pore Volume and particle size of P25 titania on the phase transformation of anatase to rutile, *Indian J. Chem.* 48 A (2009) 1378-1382.
- [7]. L. Gang, W. Xuewen, C. Zhigang, C. Hui-Ming, L. Gao Qing (Max), The Role of crystal phase in determining photocatalytic activity on nitrogen doped TiO₂. *Colloid Interface Sci.* 329 (2009) 331-338.
- [8]. H. Nakano, H. Hasuike, K. Kisoda, K. Nishio, T. Isshiki, H. Harima, Synthesis of TiO₂ nanocrystals controlled by means of the size of magnetic elements and the level of doping with them, *J. Phys.: Condens. Matter* 21 (2009) 064214.
- [9]. S. Mashid, M. Sasani Ghamsari, M. Afshar, S. Lahuti, Synthesis of TiO₂ nanoparticles By hydrolysis and peptization Of titaniumisopropoxide solution, *Semiconductor physics, Quant. Electron Optoelectron.* 9 (2006) 65-68.
- [10]. S. Jian, W. Xudong, Growth of rutile titanium dioxide nanowires by pulsed chemical vapour deposition, *Cryst. Growth Des.* 11 (2011) 949-954.
- [11]. N. Bahadur, K. Jian, R. Pasricha, Govind, S. Chand, Selective gas sensing response from different loading of Ag in sol-gel mesoporous titania powders. *Sensors and Actuators B* 159 (2011) 112-120.
- [12]. S. Song, T. Li, Z.Y. Pang, L. Lin, M. Lu, S. Han, Structural, Electrical and optical properties of ITO films with a thin TiO₂ seed layer prepared by RF magnetron sputtering, *Vacuum* 83 (2009) 1091-1094.

- [13] X. Shen, J. Zhang, B. Tian, Microemulsion-mediated solvothermal synthesis and photocatalytic properties of crystalline titania with controllable phases of anatase and rutile, *J. Hazard. Mater.* 192 (2011) 651- 657.
- [14]. M. Uzunova-Bujnova, R. Kralchevska, M. Milnova, R. Todorovska, D. Hristov, D. Todorovsky, Crystal structure, morphology and photocatalytic activity of modified TiO₂ films, *Catal. Today* 151 (2010) 14-20.
- [15]. T.A. Asif Ali Tahir, K.G. Nirmal Peiris, W. Upul, Enhancement of photoelectrochemical performance of AACVD-produced TiO₂ electrodes by microwave irradiation while preserving the nanostructure, *Chem. Vap. Dep.* 18 (2012) 107-111.
- [16]. Y. Tanaka, H. Sakai, T. Tsuke, Y. Uesugi, Y. Sakai, K. Nakamura, Influence of coil current modulation on TiO₂ nanoparticle synthesis using pulse-modulated induction thermal plasmas. *Thin Solid Films* 519 (2011) 7100- 7105.
- [17]. J.-K. Oh, J.-K. Lee, S.J. Kim, K.-W. Park, Synthesis of phase-and shape controlled TiO₂ nanoparticles via hydrothermal process. *J. Indust. Engg. and Chem.* 15 (2009) 270-274.
- [18]. A. Melis, L. Petra, S.C. Hopkins, P. Glenn, E. Johan vander, R. Susugna, G.Xavier, B.A. Glowacki, V.D Isabel, Deposition of photocatalytically active TiO₂ films assisted hydrothermal synthesis, *Nanotechnology* 23 (2012) 165603.
- [19]. Y. Zhang, H.Zheng, G. Liu, Y. Battaglia, Synthesis and electrochemical studies of a layered spheric TiO₂ through low temperature Solvothermal method, *Electrochem. Acta* 54 (2009) 4079-4083.
- [20]. Y. Zhao, C. Li, X. Liu, F. Gu, H. Jiang, W. Shao, L. Zhang, Y. He, Synthesis and optical properties of TiO₂ nanoparticles. *Mater. Letter.* 61 (2007) 79-83.
- [21]. C.-S. Kim, B.K. Moon, J.-H Park, B.-C Choi, H.-J. Seo, *Journal of Crystal Growth* 257 (2003) 309-315.
- [22]. D. Meng, T. Yamazaki, T. Kikuta, reparation and gas sensing properties of undoped and Pd-doped TiO₂ nanowires. *Sensors and Actuators B: Chemical*(2013)
- [23]. C.L. Yeha, S.H. Yeh, H.K. Ma, *Powder Technol.* 145(2004) 1.
- [24]. A.J. Rulison, P.F. Miquel, J.L Katz, *J. Mater. Res* (12) (1996) 3083.
- [25]. N. Bahadur, K. Jain, R. Pasricha, Govind, S. Chand, Selective gas sensing response from different loading of Ag in sol-gel mesoporous titania powders, *Sens. Actuators B Chem.* 159 (2011) 112-120.
- [26]. Y. Zhang, H. Zhang, G. Liu, V. Battaglia, Synthesis and electro chemical studies of a layered spherical TiO₂ through low temperature solvothermal method. *Electro. Acta* 54 (2009) 4079-4083.
- [27]. M.A Khan, M.S. Akhtar, O.-B Yang, Synthesis, characterization and application of sil-gel derived mesoporous TiO₂ nanoparticles for dye-sensitized solar cells. *Solar Energy* 84 (2010) 2195-2201.
- [28]. Y. Zhao, C. Li, X. Liu, F.Gu, H. Jiang, W. Shao, L. Zhang, Y. He, Synthesis and optical properties of TiO₂ nanoparticles, *Mater. Lett.* 61 (2007) 79-83.
- [29]. A.N JoseA, J.T. Juan, D. Pablo, R.P. Javier, R. Diana, I.L. Marta, *Appl. Catal.*, A Gen. 178 (1999) 91. [30]. S. -A. Gao, A.-P. Xian, L.-H. Cao, R.-C. Xie, J.-K. Zhang, Influence of calcining temperature on photoresponse TiO₂ film under nitrogen and oxygen in room temperature, *Sens. Actuators B Chem.* 134 (2008) 718-726.
- [31]. R. Branek, H. Kisch, *Photochem. Photobiol. Sci* 7 (2008) 40.
- [32]. J.I. Pankov, *Optical Processes in Semiconductors*, Prentice-Hall Inc., New Jersey, 1971.
- [33]. H. Tang, K. Prasad, R. Sanilines, P.E. Schmid, F. Levy, *J. Appl. Phys.* 75 (1994) 2042.
- [34]. S. Sugapriya, R. Sriram, S. Lakshmi, Effect of annealing on TiO₂ nanoparticles, *Optik* 24 (2013) 4971-4975.
- [35]. L.V. Saraf, S.I. Patil, S.B. Ogalae, S.R. Sainkar, S.T. Kshirsager, *Int. J. Mod. Phys. B*12 (1998) 2635.
- [36]. L. Fross, M. Schubnell, *Appl. Phys. B: Photophys. Laser chem.* 56 (1993) 363.
- [37]. H. Tang, H. Berger, P.E. Schmid, F. Levy, *Solid State Commun.* 87 (1993) 847.